

Normalized Power Variance: A new Field Orthogonal to Power in EEG Analysis

Clinical EEG and Neuroscience
1–9
© EEG and Clinical Neuroscience
Society (ECNS) 2022
Article reuse guidelines:
sagepub.com/journals-permissions
DOI: 10.1177/15500594221088736
journals.sagepub.com/home/eeg



Yasunori Aoki^{1,2} , Hiroaki Kazui³, Roberto D. Pascual-Marqui⁴,
Ricardo Bruña^{5,6} , Kenji Yoshiyama¹, Tamiki Wada¹,
Hideki Kanemoto¹, Yukiko Suzuki¹, Takashi Suehiro¹, Yuto Satake¹,
Maki Yamakawa¹, Masahiro Hata¹, Leonides Canuet⁷, Ryouhei Ishii^{1,8} ,
Masao Iwase¹, and Manabu Ikeda¹

Abstract

To date, electroencephalogram (EEG) has been used in the diagnosis of epilepsy, dementia, and disturbance of consciousness via the inspection of EEG waves and identification of abnormal electrical discharges and slowing of basic waves. In addition, EEG power analysis combined with a source estimation method like exact-low-resolution-brain-electromagnetic-tomography (eLORETA), which calculates the power of cortical electrical activity from EEG data, has been widely used to investigate cortical electrical activity in neuropsychiatric diseases. However, the recently developed field of mathematics “information geometry” indicates that EEG has another dimension orthogonal to power dimension — that of normalized power variance (NPV). In addition, by introducing the idea of information geometry, a significantly faster convergent estimator of NPV was obtained. Research into this NPV coordinate has been limited thus far. In this study, we applied this NPV analysis of eLORETA to idiopathic normal pressure hydrocephalus (iNPH) patients prior to a cerebrospinal fluid (CSF) shunt operation, where traditional power analysis could not detect any difference associated with CSF shunt operation outcome. Our NPV analysis of eLORETA detected significantly higher NPV values at the high convexity area in the beta frequency band between 17 shunt responders and 19 non-responders. Considering our present and past research findings about NPV, we also discuss the advantage of this application of NPV representing a sensitive early warning signal of cortical impairment. Overall, our findings demonstrated that EEG has another dimension — that of NPV, which contains a lot of information about cortical electrical activity that can be useful in clinical practice.

Keywords

normalized power variance, electroencephalography (EEG), information geometry, idiopathic normal pressure hydrocephalus, early warning signal

Received October 13, 2021; accepted February 28, 2022.

Introduction

Electroencephalogram (EEG) noninvasively measures brain cortical electrical activity at a high sampling rate (500–1000 Hz) via electrodes placed on the scalp. In the cerebral cortex, neurons connect with other surrounding neurons via synapses and collectively give rise to electrical activity, which can be detected as EEG waves by these electrodes. Hans Berger, a German psychiatrist, first recorded human EEG in 1924 and dedicated many years to his studies before proving that EEG stems from brain electrical activity, rather than artifacts.¹ Finally, EEG gained widespread recognition and visual inspection of EEG waves has been used to support diagnoses of epilepsy, dementia, and disturbance of consciousness ever since. Owing to its high temporal resolution (1–2 milliseconds), EEG contains a large amount of information about cortical electrical activities. However, most of this information

¹Department of Psychiatry, Graduate School of Medicine, Osaka University, Osaka, Japan

²Department of Psychiatry, Nippon Life Hospital, Osaka, Japan

³Department of Neuropsychiatry, Kochi Medical School, Kochi University, Kochi, Japan

⁴The KEY Institute for Brain-Mind Research, University Hospital of Psychiatry, Zurich, Switzerland

⁵UCM-UPM Centre for Biomedical Technology, Laboratory of Cognitive and Computational Neuroscience, Complutense University of Madrid, Madrid, Spain

⁶Department of Electrical Engineering, La Laguna University, Tenerife, Spain

⁷Neurology department, Nuestra Señora del Rosario hospital, Madrid, Spain

⁸Graduate School of Comprehensive Rehabilitation, Osaka Prefecture University, Osaka, Japan

Corresponding Author:

Yasunori Aoki, Department of Psychiatry, Osaka University Graduate School of Medicine, D3 2-2 Yamada-oka, Suita, Osaka 565-0871, Japan.
Email: mi_kotoginn@yahoo.co.jp

cannot be identified by visual inspection and, therefore, it is necessary to use various analysis methods (as outlined below) to extract it. Electrical activities are generated from each cerebral cortex and their linear mixture is captured by the electrodes on the scalp. So, it is necessary to estimate cerebral electrical activity from the EEG waves by solving a linear inverse problem. More specifically, discrete Fourier transform is applied, such that the EEG data recorded on electrodes are transformed into electrode position \times frequency data. The linear inverse problem is then solved by multiplying this data by a spatial filter matrix, thereby achieving conversion of the electrode position \times frequency data into cerebral cortex position \times frequency data (source estimation method).^{2,3} Exact low-resolution brain electromagnetic tomography (eLORETA) is a source estimation method that can reconstruct cortical electrical activity from EEG data with correct localization.^{2,4–6} Therefore, power analysis with eLORETA has been widely used, providing valuable results in neuroimaging studies.^{4,7–9}

Approaching EEG analysis from a different mathematical perspective, the cortical electrical activity approximately follows a specific type of probability distribution (namely, gamma distribution),¹⁰ so EEG analysis can be considered from the point of view of “information geometry”. This recently developed mathematical field allows a probability distribution to be assigned to a Riemannian manifold equipped with a metric tensor, facilitating the investigation of probability distributions by means of geometry.¹¹ Information geometry indicates that cortical electrical activity has two orthogonal dimensions, namely, normalized power variance (NPV) and Power — and we can calculate a metric tensor and distance between probability distributions in these dimensions (NPV and Power) on the Riemannian manifold.¹² In addition, by applying a maximum likelihood estimation technique, a closed-form estimator of NPV was obtained, which converges to the true value significantly faster than is the case with a classical moment estimator.¹³

From the point of view of thermal and statistical physics, NPV sensitively reflects the instability of cortical electrical activity and can be an early warning signal of phase transition of the cortical electrical activity from the healthy state to the disease state.¹⁴ In previous studies, we applied the moment estimator of NPV to EEG data in epilepsy and showed the high sensitivity of NPV with regard to the instability of cortical electrical activity at the epileptogenic electrode in the pre-seizure period and its stabilization after phase transition to the seizure period.¹⁵ We also applied the moment estimator of NPV to eLORETA source estimated data in patients of idiopathic normal pressure hydrocephalus (iNPH) prior to a cerebrospinal fluid (CSF) shunt operation. Our results indicated that there was a significant difference between shunt responders and non-responders appearing in NPV at the high-convexity area in the beta frequency band, but not in Power of eLORETA.¹⁶

In the present study, using information geometry, we demonstrated that the cortical electrical activity has another dimension —that of NPV— in addition to the Power dimension

(as outlined in Methods). Traditional neuroimaging techniques such as fMRI, SPECT, and EEG power analysis only measured information in the Power dimension. We therefore explored whole dimensions (NPV and Power) of eLORETA cortical electrical activity using the closed-form estimator in iNPH patients prior to a CSF shunt operation and aimed to find presurgical differences in cortical electrical activity that associated with the CSF shunt operation outcome — a feat that traditional neuroimaging techniques have failed to achieve.^{16,17} Our findings indicate that NPV analysis represents a new field in EEG analysis, providing a great deal of useful information to be used in clinical practice and facilitating greater understanding of the mechanisms of neuropsychiatric diseases.

Methods

Subjects

Right-handed definite and probable iNPH patients were consecutively recruited from the Neuropsychology Clinic at the Department of Psychiatry in Osaka University Hospital. The iNPH patients underwent a CSF shunt operation at the Department of Neurosurgery in Osaka University Hospital between April 2010 and February 2021. The inclusion and exclusion criteria for definite and probable iNPH patients complied with Japanese diagnostic criteria for iNPH (further details can be found in our previous study).¹⁸ All of the included patients showed the morphological feature of a disproportionately enlarged subarachnoid-space hydrocephalus on head MRI findings, as defined in Japanese diagnostic criteria for iNPH.¹⁷ CSF tap test and the CSF shunt operation were performed in accordance with the Japanese Clinical Guidelines for iNPH.¹⁷

Out of 47 patients who met the inclusion criteria, three patients were excluded due to comorbidity of Parkinson’s disease or parkinsonian syndrome; two patients due to long-standing overt ventriculomegaly on head MRI findings; five patients due to the lack of 500-second (500-s) artifact-free segments; and one patient that did not complete the follow-up after the CSF shunt operation. As a result, a total of 36 patients were included in the present study.

This study was approved by the Ethics Committee of Osaka University Hospital and written informed consent was obtained from patients or their families.

Assessment of Gait and Cognition

Assessments of gait and cognition have already been described in our previous study.¹⁸ Briefly, gait disturbance was assessed by the Gait Status Scale-Revised (GSSR),¹⁹ the 10-metre reciprocating walking test (WT), and the 3-metre Timed Up and Go (TUG) test.²⁰ The thresholds of improvement were set at 1-point improvement in the GSSR and 10% improvement in the WT and TUG. Improvement in all gait tests was considered clinical improvement in gait.

Cognitive impairment was assessed using the Frontal Assessment Battery (FAB),²¹ Mini-Mental State Examination (MMSE),²² Wechsler Adult Intelligence Scale-III (WAIS-III)-Block Design, WAIS-III-Digit Symbol Coding,²³ Wechsler Memory Scale-Revised (WMS-R)-Attention/Concentration Index,²⁴ and Trail Making Test Part A (TMT-A).²⁵ The improvement thresholds of the cognitive tests were set at 2, 3, 3, 3, 15 points, and 30%, respectively. Improvement in more than half of the cognitive tests was considered clinical improvement in cognition.

Assessment of CSF Shunt Operation Outcome

The method of assessment of the outcome of the CSF shunt operation has already been described in our previous study.¹⁸ Briefly, gait and cognitive symptoms were evaluated 1 to 3 months before the CSF shunt operation — and again 1, 3, 6 months and 1 year after the operation. CSF shunt operation outcome was deemed positive if gait or cognition had clinical improvement at any time of postsurgical evaluations; otherwise, it was deemed negative. Accordingly, the patients were classified into responders and non-responders to the CSF shunt operation. These classification criteria were stricter than those of the Japanese Clinical Guidelines for iNPH¹⁷ as we only selected those patients that had shown a significant improvement in symptoms as shunt responders.¹⁸

EEG Data Acquisition

The EEG data acquisition, eLORETA and eLORETA-NPV analysis procedures have already been described in detail in our previous studies.^{4,16} Briefly, EEG data was recorded during resting state with eyes closed for about 20 minutes 1 to 3 months before the CSF shunt operation, using a 19-electrode EEG system (EEG-1000/EEG-1200, Nihon Kohden Inc., Tokyo, Japan) with a sampling rate of 500 Hz, and filtered through a band-pass filter of 0.53–120 Hz. The subjects were instructed to relax in the bed but stay awake. During the EEG recordings, drowsiness was avoided by repeating the instructions. Then, 500-s artifact-free segments were selected offline by visual inspection for each patient, the band-pass filter setting was changed to 1.6–60 Hz, and the segments were imported into the eLORETA and eLORETA-NPV analyses.

eLORETA and eLORETA-NPV Analyses

eLORETA is a linear weighted minimum norm inverse solution which has the property of correct localization albeit with low spatial resolution.^{2,3} The solution space consists of 6239 voxels in the cortical grey matter at 5 mm spatial resolution, in a realistic head model²⁶ with the MNI152 template.²⁷ The eLORETA method has been widely used to investigate cortical electrical activities and it has been validated through studies of neuropsychiatric diseases and human data during various

sensory stimulations.^{4–6,28,29} In the present study, eLORETA and eLORETA-NPV analyses were performed in MATLAB R2021a software. In these analyses, for each subject, 500-s EEG data from 19 electrodes were re-referenced to the average reference to reduce diffuse artifacts covering all electrodes. EEG data were transformed into frequency data as electrode position × time × frequency matrix by discrete Fourier transform with rectangular window using time-frequency analysis (ft_freqanalysis) in Field Trip toolbox (<http://www.fieldtriptoolbox.org/>) installed in the MATLAB software. The frequency data were then transformed to the cortical electrical current density data as cerebral cortex position × time × frequency matrix by multiplying the spatial filter of eLORETA. The spatial filter of eLORETA was calculated using the MATLAB program written by author R. B., which followed a technical instruction about eLORETA provided by author R. D. P.-M.³ Finally, the cortical electrical activity was obtained by squaring the cortical electrical current density and averaging over the entire EEG segment. In eLORETA-NPV analysis, NPV of cortical electrical activity for each 4.6 s EEG segment was calculated and averaged over the entire EEG segment, where NPV was defined as variance of cortical electrical activity divided by the square of mean cortical electrical activity. The eLORETA and eLORETA-NPV analyses were computed for five frequency bands: delta (3.0–4.0 Hz), theta (4.5–7.0 Hz), alpha (7.5–13.0 Hz), beta (13.5–29.5 Hz), and gamma (30.0–40.0 Hz).

Information Geometry About Cortical Electrical Activity

The cortical electrical activity at each cortical voxel in each frequency band approximately follows gamma distribution.¹⁰

$$f(x) = \frac{1}{\Gamma(\kappa)\theta^\kappa} x^{\kappa-1} e^{-\frac{x}{\theta}} \quad \text{for } x > 0 \quad \kappa, \theta > 0$$

where Γ is a gamma function.

This gamma distribution is a probability distribution parameterized by a shape parameter κ and a scale parameter θ . Interestingly, this shape parameter κ corresponds to 1/NPV. Information geometry defines “Divergence”, which is a weaker notion of distance between probability distributions, as similar distributions have small divergence and different distributions have large divergence. According to the Divergence, probability distributions are assigned to certain coordinates on the Riemannian manifold, whose geometry is characterized by a metric tensor. The metric tensor, which can be calculated from the second derivative of log-normalizer, induces an inner product space that allows us to measure lengths and angles between tangent vectors. In our study, we selected mixed parametrization of natural and dual parametrization as $(\kappa = \frac{1}{NPV}, E(x) = \kappa\theta)$ where $E(x)$ means expected value of power. The metric tensor g of gamma distribution for this

mixed parametrization is as shown below.

$$g = \begin{bmatrix} \psi_1(\kappa) - \frac{1}{\kappa} & 0 \\ 0 & \frac{1}{\kappa\theta^2} \end{bmatrix}$$

where ψ_1 is a trigamma function.^{11,12}

Then, we can see that the inner product between the 1/NPV parameter and the Power parameter is zero, which indicates that mixed parametrization is orthogonal. This also indicates that NPV itself and Power can be orthogonal on the Riemannian manifold. However, with this parametrization (NPV, Power), it is difficult to calculate Divergence manually, so we took the parametrization of (1/NPV, Power) for the Divergence calculation. Symmetrized Bregman Divergence between distribution p and q can be calculated from the metric tensor g as follows:

$$\text{Divergence} = \left(\oint_{x_q}^{x_p} dx g \right) \cdot (x_p - x_q)$$

where x_p , x_q are coordinates of distribution p and q on the Riemannian manifold.¹¹

Thus, symmetrized Bregman Divergence between $(\kappa_1, \kappa_1\theta_1)$ and $(\kappa_2, \kappa_1\theta_1)$ was calculated as:

$$\begin{aligned} \text{Divergence} (\kappa_1, \kappa_1\theta_1 \leftrightarrow \kappa_2, \kappa_1\theta_1) \\ = \left[\psi(\kappa_2) - \psi(\kappa_1) + \log \frac{\kappa_1}{\kappa_2} \right] (\kappa_2 - \kappa_1) \end{aligned}$$

where ψ is a digamma function.

Symmetrized Bregman Divergence between $(\kappa_2, \kappa_1\theta_1)$ and $(\kappa_2, \kappa_2\theta_2)$ was calculated as:

$$\begin{aligned} \text{Divergence} (\kappa_2, \kappa_1\theta_1 \leftrightarrow \kappa_2, \kappa_2\theta_2) \\ = \kappa_2 \left(\frac{1}{\kappa_1\theta_1} - \frac{1}{\kappa_2\theta_2} \right) (\kappa_2\theta_2 - \kappa_1\theta_1) \end{aligned}$$

Then, symmetrized Bregman Divergence between $(\kappa_1, \kappa_1\theta_1)$ and $(\kappa_2, \kappa_2\theta_2)$ was calculated as shown below (since the Pythagorean Theorem holds for Divergence):

$$\begin{aligned} \text{Divergence} (\kappa_1, \kappa_1\theta_1 \leftrightarrow \kappa_2, \kappa_2\theta_2) \\ = \text{Divergence} (\kappa_1, \kappa_1\theta_1 \leftrightarrow \kappa_2, \kappa_1\theta_1) \\ + \text{Divergence} (\kappa_2, \kappa_1\theta_1 \leftrightarrow \kappa_2, \kappa_2\theta_2) \end{aligned}$$

Closed-Form Estimator of NPV and θ

We adopted a closed-form estimator of NPV and θ , which were previously obtained by applying maximum likelihood estimation to a generalized gamma distribution.¹³ The great advantage of this is that it allows a significantly faster convergence to the

true value than with a classical moment estimator, which we used in a previous study.^{13,16}

We also adopted bias correction to obtain unbiased estimators of NPV and θ , as follows¹³:

$$\frac{n}{n-1} E(\widehat{NPV}) = NPV, \quad \frac{n}{n-1} E(\widehat{\theta}) = \theta$$

where n is a number to be averaged, \widehat{NPV} and $\widehat{\theta}$ are closed-form estimators, and NPV and θ are their true values.

Statistical Group Analysis

Before statistical comparison, the eLORETA cortical electrical activity of each subject was normalized by dividing by its mean value over whole cortical voxels and frequency bands to lessen subject-wise differences in cortical electrical activity (subject-wise normalization). We measured the statistical group difference of the eLORETA cortical electrical activity between shunt responders and non-responders at each cortical voxel in each frequency band using G-test with the symmetrized Bregman Divergence calculated above.³⁰ The level of significance for the G-test was set at $P < .05$ with multiple comparison correction across 6239 cortical voxels using a permutation test.³¹ MATLAB program of this statistical group analysis using G-test with the symmetrized Bregman Divergence has been provided (Algorithm in Supplemental Material). Gamma distribution of eLORETA cortical electrical activity of each frequency band followed different shape and scale parameters; therefore, we applied the permutation test to the 6239 cortical voxels but not to the five frequency bands.

Results

Demographic and Clinical Results

Based on the CSF shunt operation outcome, 36 right-handed iNPH patients were classified into 17 shunt responders and 19 non-responders. Almost all of the shunt responder patients had improvement in the gait function only, while one patient had both gait and cognitive improvement and two patients had cognitive improvement only. Table 1 displays demographic and clinical characteristics of the subjects, showing that there was no significant difference between shunt responders and non-responders regarding gender, age, and initial clinical scores. The ratio of shunt responders to non-responders was relatively low, as our classification criteria for the CSF shunt operation outcome were stricter than those of the Japanese Clinical Guidelines, in order to classify patients that had shown significant improvements in gait or cognition as shunt responders.¹⁸

eLORETA-NPV Analysis Results

There was a significant difference in location along the NPV axis on the Riemannian manifold between shunt responders and non-responders in eLORETA cortical electrical activities

Table I. Cognitive and Gait Function Test Scores of Shunt Responders and Non-Responders.

Test	Shunt responders	Non-responders	P-value
Gender (F/M)	7/10	8/11	.95
Age	76.0 ± 6.0	76.0 ± 6.0	.75
WT	26.6 ± 18.5	21.8 ± 6.3	.36
TUG	15.6 ± 5.5	13.7 ± 4.9	.27
GSSR	7.1 ± 3.2	6.0 ± 2.0	.21
MMSE	23.4 ± 4.1	24.4 ± 3.9	.44
FAB	11.2 ± 2.6	11.8 ± 2.6	.45
TMT-A	110 ± 76	105 ± 90	.86
WMS-R_Attention/ Concentration index	82.4 ± 16.4	85.7 ± 12.1	.50
WAIS-III-Digit Symbol-Coding	6.5 ± 2.9	7.2 ± 2.6	.51
WAIS-III-Block Design	6.9 ± 3.0	7.3 ± 2.1	.67

Data are mean ± SD. Difference in the female to male ratios between shunt responders and non-responders was assessed using Chi-square test. Differences in the other scores are assessed using independent Student's t-test (uncorrected). WT: 10-m reciprocating walking test, TUG: 3 m Timed Up and Go, GSSR: Gait Status Scale-Revised, MMSE: Mini-Mental State Examination, FAB: Frontal Assessment Battery, TMT-A: Trail Making Test Part A, WMS-R: Wechsler Memory Scale-Revised, WAIS-III: Wechsler Adult Intelligence Scale-III.

measured by G-test with the symmetrized Bregman Divergence. Specifically, shunt responders had significantly higher NPV values of cortical electrical activity compared to non-responders at the high-convexity area (ie, cingulate gyrus, paracentral lobule, and medial frontal gyrus) in the beta frequency band, as shown in Figures 1 to 3 [extreme $P = .016$ at the paracentral lobule ($X = 5$, $Y = -15$, $Z = 50$ (mm); MNI coordinates)].

eLORETA Power Analysis Results

There was no significant difference in location along the power axis on the Riemannian manifold between shunt responders and non-responders. In addition, there was no significant difference between shunt responders and non-responders with regard to the location in the whole space on the Riemannian manifold.

Discussion

Information geometry demonstrated that the cortical electrical activity has another dimension in addition to the Power dimension on the Riemannian manifold — that of NPV. Given that this point had so far received little attention, in the present study we investigated whole dimensions (NPV and Power) of cortical electrical activity using eLORETA with the closed-form estimator of NPV in iNPH patients prior to them having a CSF shunt operation. Our main finding was that a significant difference in location between shunt responders and non-

responders resided only along the NPV dimension —but not along the Power dimension— on the Riemannian manifold.

In a previous study, using eLORETA analysis with the classical moment estimator of NPV, we found that shunt responders had significantly higher NPV values at the high-convexity area in the beta frequency band compared to non-responders (extreme P at $X = 5$, $Y = -15$, $Z = 45$ (mm); MNI coordinates).¹⁶ In the present study, eLORETA analysis with the closed-form estimator of NPV demonstrated almost the same spatial configuration of NPV in shunt responders and non-responders (Figures 1, 2) and detected a significant difference in NPV between shunt responders and non-responders at almost the same cortical point (extreme P at $X = 5$, $Y = -15$, $Z = 50$ (mm); MNI coordinates) (Figure 3). In a previous study, we used the classical moment estimator of NPV and employed a moving average filter method to compensate for the slow convergence of the moment estimator. In the present study, the fact that the eLORETA analysis with the closed-form estimator of NPV obtained practically the same results without using the moving average filter method suggests that the closed-form estimator of NPV has significantly faster convergence than the moment estimator previously demonstrated by Zhi-Sheng and Nan.¹³

From the perspective of thermal and statistical physics, NPV sensitively reflects the instability of cortical electrical activity and detects early changes in cortical electrical activity prior to phase transition from the healthy state to the disease state.¹⁴ Musha who is renowned for his 1/f fluctuation research, reported that NPV analysis of EEG data could identify pre-Alzheimer's disease patients (who later developed Alzheimer's disease in 12-18 months) from healthy subjects with a low false positive rate of 15%.³² We also applied NPV analysis to EEG data in epilepsy and showed sensitive detectability of NPV, visualizing the early surge of NPV value at the epileptogenic electrode prior to seizure onset.¹⁵ In addition, we applied eLORETA-NPV with the moment estimator to EEG data of iNPH patients prior to them having CSF shunt operation and found a significant difference in NPV between shunt responders and non-responders at the high-convexity area.¹⁶ The high-convexity area is compressed by dilated ventricles with accumulated CSF is an area that is attracting attention due to its association with responsiveness to CSF shunt operation.³³⁻³⁵ These past results, taken together with our present findings, suggest that NPV has the capacity for the early detection of cortical impairment prior to phase transition from the healthy state to the disease state or from reversible state to irreversible state for treatment.

From the perspective of information geometry, the cortical electrical activity has two orthogonal dimensions —NPV and Power— on the Riemannian manifold, as outlined in Methods. Traditional EEG power analysis methods have only measured power dimension information of the cortical electrical activity. Other neuroimaging methods such as fMRI PET and SPECT measure secondary hemodynamic and metabolic changes to the neuronal activity with high spatial resolution,

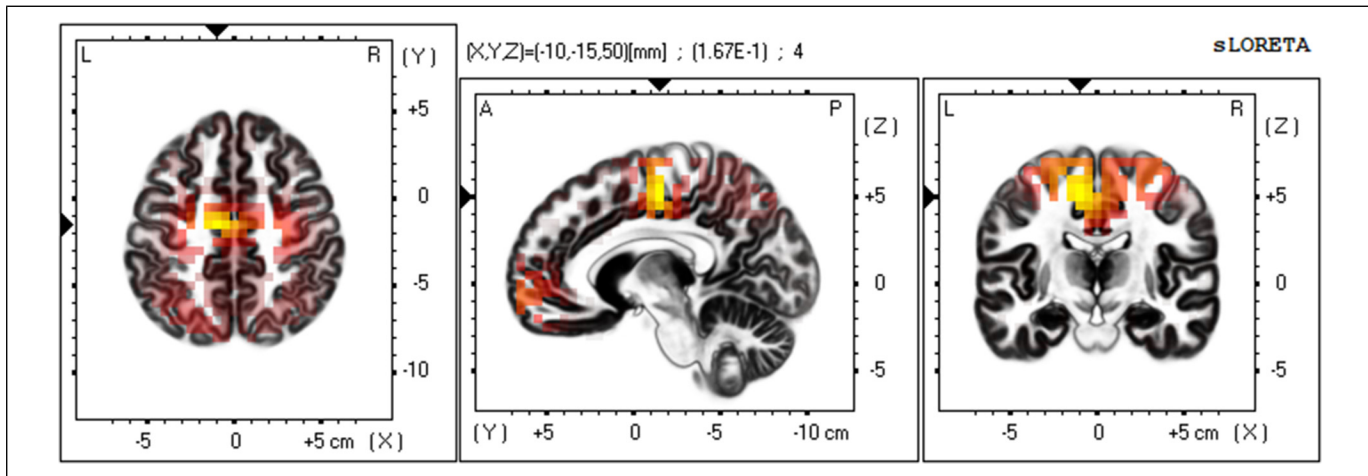


Figure 1. Mean eLORETA-NPV values of 17 shunt responders in the beta frequency band. Normalized power variance (NPV) of eLORETA cortical electrical activity is color coded from grey (zero) to red to bright yellow (maximum). Slices from left to right are axial, sagittal, and coronal images (viewed from top, left and back). L, left; R, right; A, anterior; P, posterior.

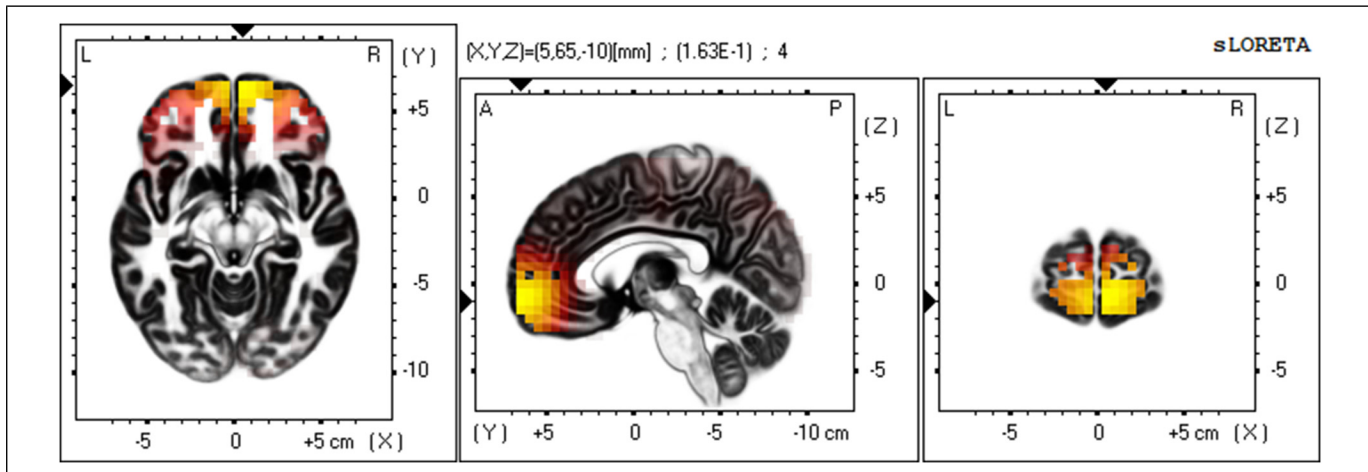


Figure 2. Mean eLORETA-NPV values of 19 non-responders in the beta frequency band. Normalized power variance (NPV) of eLORETA cortical electrical activity is color coded from grey (zero) to red to bright yellow (maximum). Slices from left to right are axial, sagittal, and coronal images (viewed from top, left and back). L, left; R, right; A, anterior; P, posterior.

albeit at low temporal resolution, and thus contain almost exclusively power dimension information of the neuronal activity. In this study, using the symmetrized Bregman Divergence, we observed a significant distance between shunt responders and non-responders along the NPV dimension—but not along the Power dimension—on the Riemannian manifold, which indicates the importance of exploring whole dimensions of cortical electrical activity.

Brain aging occurs due to the accumulation of age-related physiological changes in the brain neuronal population. In a previous study, using NPV analysis, we investigated age-related changes in healthy individuals and found that the levels of NPV of cortical electrical activity increased from the young to middle-aged group and decreased from the middle-aged to the elderly group.³⁶ In addition, past EEG and fMRI

studies investigated age-related changes in cortical electrical activity and cerebral blood flow and showed a decrease in power during aging with both linear and nonlinear trends.^{7,37} Taking into account both past and present findings, we propose a hypothesis that accumulated impairment of cortical electrical activity first manifests as an increase in the NPV value prior to phase transition from the healthy state to the disease state and then as a decrease in the Power value after the phase transition to the disease state (Figure 4).

The present study demonstrated that, unlike other neuroimaging methods such as SPECT, PET, fMRI, and traditional EEG power analysis and eLORETA power analysis that have been used to explore brain activity, eLORETA-NPV analysis had the capacity to sensitively detect changes in fluctuations of cortical electrical activities associated with CSF shunt

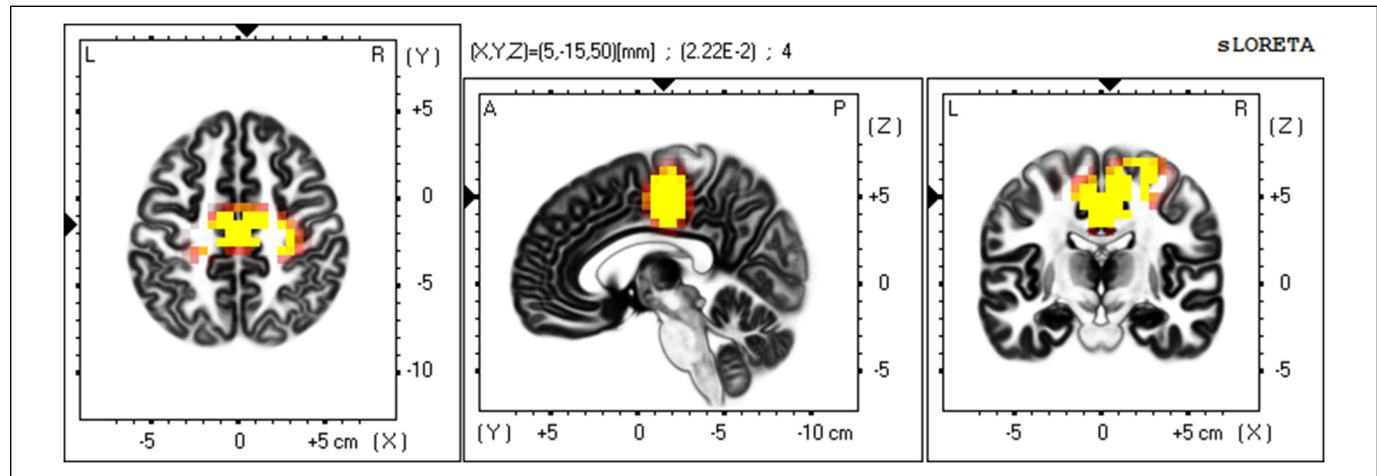


Figure 3. The significant difference in the normalized power variance (NPV) of eLORETA cortical electrical activity—between 17 shunt responders and 19 non-responders—in the beta frequency band, measured by G-test with the symmetrized Bregman Divergence. Shunt responders had significantly higher NPV values of cortical electrical activity in the beta frequency band at the high-convexity area compared to non-responders [extreme $P=.016$ at the paracentral lobule ($X=5$, $Y=-15$, $Z=50$ (mm); MNI coordinates)]. The symmetrized Bregman Divergence above threshold ($P<.05$) is color coded from red to bright yellow (maximum). Slices from left to right are axial, sagittal, and coronal images (viewed from top, left and back). L, left; R, right; A, anterior; P, posterior.

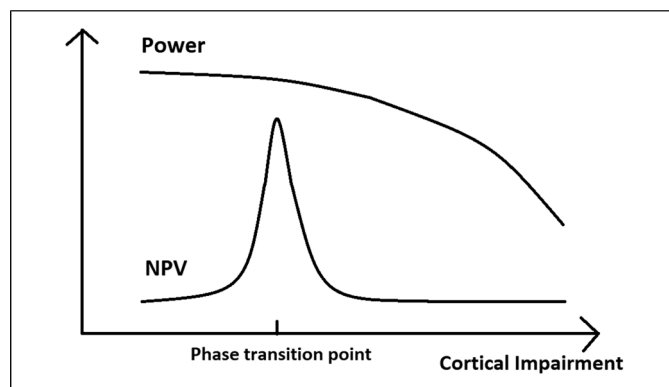


Figure 4. Hypothesis regarding changes in NPV and Power of cortical electrical activity for accumulated cortical impairment. Impaired cortical electrical activity first manifests as an increase in NPV value prior to phase transition from the healthy state to the disease state and then as a decrease in Power value after the phase transition to the disease state.

response at the high-convexity area in iNPH. This may be attributed to the following: (i) EEG directly detects cortical electrical activity with high temporal resolution (1-2 ms); (ii) eLORETA reconstructs cortical electrical activity from EEG data with correct localization; and (iii) NPV sensitively detects instability of cortical electrical activity. Our results, together with those of previous studies, suggest that eLORETA-NPV analysis is a useful and sensitive tool to assess cortical states, providing valuable information regarding the early detection of neuropsychiatric diseases and prediction of therapeutic effect.

It should be noted that our results should be interpreted with caution since the sample size of iNPH patients was relatively

small. Therefore, our findings should be considered as preliminary, and would need to be confirmed in larger samples. Nevertheless, our finding of NPV changes related to the CSF shunt response is in accordance with previous neuroimaging findings in iNPH patients.^{16,33-35} This leads us to suggest that eLORETA-NPV with the closed-form estimator is a reliable method of detecting instability of cortical electrical activity.

Conclusion

Overall findings indicate that NPV is an independent dimension orthogonal to Power and it will also contain a great deal of information about cortical electrical activity. While the classical moment estimator of NPV was problematic given the slow convergence to the true value, this issue was significantly improved by the closed-form estimator of NPV. Furthermore, eLORETA-NPV has the advantage of being a sensitive early warning signal of cortical impairment. Therefore, eLORETA-NPV analysis with the closed-form estimator is a powerful and promising tool to assess and predict brain cortical states in patients with various neuropsychiatric diseases.

Acknowledgments

We are grateful to Prof. Haruhiko Kishima and staff members of the Department of Neurosurgery in Osaka University Hospital, who performed CSF shunt operations.

Author Contributions

Y.A., Hiroaki K., and R.I. designed the study. Y.A. wrote an eLORETA-NPV program, analysed the EEG data and wrote the manuscript. R.D.P.-M. and R.B. provided the eLORETA program and gave technical advice about it and the Field Trip toolbox. H.K.,

K.Y., T.W., H.K., Y.S., T.S., Y.S., and M.Y. recruited subjects, performed CSF tapping and assessed their symptoms. All authors reviewed the manuscript.

Availability of Data

Data to reproduce the results of this study are available from the corresponding author.

Code Availability

The code of statistical group analysis using G-test with the symmetrized Bregman Divergence is provided (Algorithm in Supplemental Material).

Declaration of Conflicting Interests

The author(s) declared no potential conflicts of interest with respect to the research, authorship, and/or publication of this article.

Ethical Approval

Not applicable, because this article does not contain any studies with human or animal subjects.

Research Ethics and Patient Consent

This study was approved by the Ethics Committee of Osaka University Hospital. Written informed consent was obtained from patients or their families.

Funding

This study was supported by the following funding from the Research Committee of Normal Pressure Hydrocephalus and Related Disorders: (i) grants for studies focusing on etiology, pathogenesis and therapy from the Japanese Ministry of Health, Labour and Welfare (Tokyo, Japan) (08069915, 11103508, 14428046) and (ii) a grant for studies into the creation of Japanese Clinical Guidelines for iNPH from the Japanese Ministry of Health, Labour and Welfare (Tokyo, Japan) (17933261).

This study was supported by the following grants from the Japan Agency for Medical Research and Development: (i) “Study into the possibility of hydrocephalus treatment by elimination of amyloid- β in the brain (16K10212)”; (ii) “Study into the prediction of the effect of surgery in patients with idiopathic normal pressure hydrocephalus (24591710)”; (iii) “Development and validation of artificial intelligence to detect and classify prodromal dementia using EEG in resting state (JP20de0107001)”; and (iv) “Study of optimization of epilepsy treatment using artificial intelligence (Brain/MINDS Beyond; JP23m0307103)”.

This study was also supported by the following grant from Sugita Memorial Brain Research Grant Funding: “Study into gait disturbance in patients with idiopathic normal pressure hydrocephalus”.

ORCID iDs

Yasunori Aoki  <https://orcid.org/0000-0003-0488-538X>
 Ricardo Bruña  <https://orcid.org/0000-0003-1007-900X>
 Ryouhei Ishii  <https://orcid.org/0000-0002-4245-0953>

Supplemental Material

Supplemental material for this article is available online.

References

- Gloor P. Hans Berger and the discovery of the electroencephalogram. *Electroencephalogr Clin Neurophysiol*. 1969;28 (Suppl 28):1-36.
- Grech R, Cassar T, Muscat J, et al. Review on solving the inverse problem in EEG source analysis. *J Neuroeng Rehabil*. 2008;5:25. doi:10.1186/1743-0003-5-25
- Pascual-Marqui RD. Discrete, 3D distributed, linear imaging methods of electric neuronal activity. Part 1: exact, zero error localization. arXiv. 0710.3341 [math-ph]. 2007 October-17. <http://arxiv.org/pdf/0710.3341>
- Aoki Y, Ishii R, Pascual-Marqui RD, et al. Detection of EEG-resting state independent networks by eLORETA-ICA method. *Front Hum Neurosci*. 2015;9(31). doi:10.3389/fnhum.2015.00031
- Pascual-Marqui RD, Faber P, Kinoshita T, et al. Comparing EEG/MEG neuroimaging methods based on localization error, false positive activity, and false positive connectivity. bioRxiv. 2008. doi:<https://doi.org/10.1101/269753>
- Pascual-Marqui RD, Lehmann D, Koukkou M, et al. Assessing interactions in the brain with exact low-resolution electromagnetic tomography. *Philos Trans A Math Phys Eng Sci*. 2011;369(1952):3768-3784. doi:10.1098/rsta.2011.0081
- Babiloni C, Binetti G, Cassarino A, et al. Sources of cortical rhythms in adults during physiological aging: a multicentric EEG study. *Hum Brain Mapp*. 2006;27(2):162-172. doi:10.1002/hbm.20175
- Babiloni C, Del Percio C, Lizio R, et al. Abnormalities of resting-state functional cortical connectivity in patients with dementia due to Alzheimer’s and Lewy body diseases: an EEG study. *Neurobiol Aging*. 2018;65:18-40. doi:10.1016/j.neurobiolaging.2017.12.023
- Canuet L, Ishii R, Pascual-Marqui RD, et al. Resting-state EEG source localization and functional connectivity in schizophrenia-like psychosis of epilepsy. *PLoS One*. 2011;6(11):e27863. doi:10.1371/journal.pone.0027863
- Thatcher RW, North D, Biver C. Evaluation and validity of a LORETA normative EEG database. *Clin EEG Neurosci*. 2005;36(2):116-122. doi:10.1177/155005940503600211
- Amari S, Nagaoka H. *Methods of information geometry*. American Mathematical Society/Oxford University Press; 2000.
- Nielsen F. An elementary Introduction to information geometry. *Entropy (Basel)*. 2020;22(10):1100. doi:10.3390/e22101100
- Zhi-Sheng YE, Nan C. Closed-form estimators for the gamma distribution derived from likelihood equations. *Am Stat*. 2017;71:177-181. doi:10.1080/00031305.2016.1209129
- Chen L, Liu R, Liu ZP. Detecting early-warning signals for sudden deterioration of complex diseases by dynamical network biomarkers. *Sci Rep*. 2012;2:342. doi:10.1038/srep00342
- Aoki Y, Ishii R, Iwase M, et al. Normalized power variance change between pre-ictal and ictal phase of an epilepsy patient using NAT analysis: a case study. *Annu Int Conf IEEE Eng Med Biol Soc*. 2013;2013:437-440. doi:10.1109/EMBC.2013.6609530
- Aoki Y, Kazui H, Bruña R, et al. Normalized power variance of eLORETA at high-convexity area predicts shunt response in idiopathic normal pressure hydrocephalus. *Sci Rep*. 2020;10(1):13054. doi:10.1038/s41598-020-70035-9

17. Mori E, Ishikawa M, Kato T, et al. Guidelines for management of idiopathic normal pressure hydrocephalus: second edition. *Neurol Med Chir (Tokyo)*. 2012;52(11):775-809. doi:10.2176/nmc.52.775
18. Aoki Y, Kazui H, Tanaka T, et al. EEG and neuronal activity topography analysis can predict effectiveness of shunt operation in idiopathic normal pressure hydrocephalus patients. *Neuroimage Clin.* 2013;3:522-530. doi:10.1016/j.nicl.2013.10.009
19. Kubo Y, Kazui H, Yoshida T, et al. Validation of grading scale for evaluating symptoms of idiopathic normal-pressure hydrocephalus. *Dement Geriatr Cogn Disord.* 2008;25(1):37-45. doi:10.1159/000111149
20. Podsiadlo D, Richardson S. The timed "up & go": a test of basic functional mobility for frail elderly persons. *J Am Geriatr Soc.* 1991;39(2):142-148. doi:10.1111/j.1532-5415.1991.tb01616.x
21. Dubois B, Slachevsky A, Litvan I, et al. The FAB: a frontal assessment battery at bedside. *Neurology.* 2000;55(11):1621-1626. doi:10.1212/wnl.55.11.1621
22. Folstein MF, Folstein SE, McHugh PR. "Mini-mental state". A practical method for grading the cognitive state of patients for the clinician. *J Psychiatr Res.* 1975;12(3):189-198. doi:10.1016/0022-3956(75)90026-6
23. Wechsler D. *Wechsler Adult Intelligence Scale-Third Edition*. The Psychological Corporation; 1997.
24. Wechsler D. *Wechsler Memory Scale-Revised*. The Psychological Corporation; 1987.
25. Reitan RM. The relation of the trail making test to organic brain damage. *J Consult Psychol.* 1955;19(5):393-394. doi:10.1037/h0044509
26. Fuchs M, Kastner J, Wagner M, et al. A standardized boundary element method volume conductor model. *Clin Neurophysiol.* 2002;113(5):702-712. doi:10.1016/s1388-2457(02)00030-5
27. Mazziotta J, Toga A, Evans A, et al. A probabilistic atlas and reference system for the human brain: international consortium for brain mapping (ICBM). *Philos Trans R Soc Lond B Biol Sci.* 2001;356(1412):1293-1322. doi:10.1098/rstb.2001.0915
28. Jatoi MA, Kamel N, Malik AS. EEG Based brain source localization comparison of sLORETA and eLORETA. *Australas Phys Eng Sci Med.* 2014;37(4):713-721. doi:10.1007/s13246-014-0308-3
29. Zhang J, Huang S, Nan W, et al. Switching tinnitus-on: maps and source localization of spontaneous EEG. *Clin Neurophysiol.* 2021;132(2):345-357. doi:10.1016/j.clinph.2020.10.023
30. McDonald JH. "G-test of goodness-of-fit". *Handbook of Biological Statistics*. 3rd ed. Sparky House Publishing; 2014:53-58.
31. Nichols TE, Holmes AP. Nonparametric permutation tests for functional neuroimaging: a primer with examples. *Hum Brain Mapp.* 2002;15(1):1-25. doi:10.1002/hbm.1058
32. Musha T, Matsuzaki H, Kobayashi Y, et al. EEG Markers for characterizing anomalous activities of cerebral neurons in NAT (neuronal activity topography) method. *IEEE Trans Biomed Eng.* 2013;60(8):2332-2338. doi:10.1109/TBME.2013.2255101
33. Narita W, Nishio Y, Baba T, et al. High-convexity tightness predicts the shunt response in idiopathic normal pressure hydrocephalus. *AJNR Am J Neuroradiol.* 2016;37(10):1831-1837. doi:10.3174/ajnr.A4838
34. Virhammar J, Laurell K, Cesarini KG, et al. The callosal angle measured on MRI as a predictor of outcome in idiopathic normal-pressure hydrocephalus. *J Neurosurg.* 2014;120(1):178-184. doi:10.3171/2013.8.JNS13575
35. Virhammar J, Laurell K, Cesarini KG, Larsson EM. Preoperative prognostic value of MRI findings in 108 patients with idiopathic normal pressure hydrocephalus. *AJNR Am J Neuroradiol.* 2014;35(12):2311-2318. doi:10.3174/ajnr.A4046
36. Ishii R, Canuet L, Aoki Y, et al. Healthy and pathological brain aging: from the perspective of oscillations, functional connectivity, and signal complexity. *Neuropsychobiology.* 2018;75(4):151-161. doi:10.1159/000486870
37. Allen EA, Erhardt EB, Damaraju E, et al. A baseline for the multivariate comparison of resting-state networks. *Front Syst Neurosci.* 2011;5:2. doi:10.3389/fnsys.2011.00002